UNIVERSITY OF CRETE
DEPARTMENT OF PHYSICS

BACHELOR THESIS

Effects of shear on the microstructure and mechanical properties of colloidal gels

Vasiliki Chrysoulaki

Supervisor: George Petekidis

May 2023

Acknowlegments

I would like to express my gratitude to the following people who have supported and encouraged me throughout the process of completing this bachelor thesis. First and foremost, I would like to thank my supervisor Prof. George Petekidis for his guidance, expertise and patience throughout this project. He was very supportive in introducing me to new ideas, theories, and methodologies and for challenging me to think critically and creatively about the topic. Many thanks go also to Prof. Dimitris Vlassopoulos for all the support and the encouragement during this work.

I am also grateful to Mohan Das for teaching me and helping me in my begginings to rheology with patience and kindness. I would like to thank Antonis Mavromanolakis and Antje Larsen for using all their knowledge and experience to help me at any technical or even personal problem I had. Many thanks go also to Manos Mathioudakis for the great collaboration we had at confocal microscopy measurements and also Manos Vereroudakis, Esmaeel Moghimi, Thanasis Athanasiou, Katerina Peponaki, Nikos Burger and all the other members of the group for all the discussions and the advices they gave me during this work.

Finally, I would like to express my thanks to my parents, my family and my friends, for their understanding and support.

Abstract

The last few years, the ability to tune structural and mechanical properties of soft matter through processing has great interest at industries related to food, personal care products or ceramics etc. A suspension of colloidal hard spheres is a model soft matter system that can be used to investigate such structural changes occurring during processing. In particular, the system we study here, is a depletion gel of nearly monodisperse Poly-methyl methacrylate (PMMA) particles at large volume fraction (44%). We use rheology in combination with confocal microscopy to probe the changes in the mechanical properties and the structure under oscillatory shear at various strain amplitudes and frequencies for different durations of pre-shear. We find that such colloidal gels exhibit a drop in their elastic modulus, after shearing, that depends on the applied strain amplitude (γ_0), the shearing time and the frequency (ω) and it seems to be related with the crystallization of the gel and possibly with their approach to phase separation.

TABLE OF CONTENTS

CHAPTER 1

INTRODUCTION

Colloidal systems are mixtures of two insoluble phases in which the first consists of particles, with diameter of 10 nanometer to 10 micrometer, that are suspended in the second substance. The phase transitions of colloids are similar with atom's and molecule's, making them an interesting system for investigation as they can also be visible in an optical microscope. Moreover, colloids have various applications in many fields, such as food industries, medicinal field etc.

An interesting property of colloidal particles is their Brownian motion which arises from the random thermal collisions of the suspending medium molecules with the particles and leads to diffusive motion of the latter. The Stokes-Einstein[1] relation gives the diffusion coefficient D_0 for a colloidal particle with radius a dispersed in a solvent of viscosity η_m:

$$D_0 = k_B T / 6\pi\eta_m a$$

Furthermore, colloidal particles suspended in a liquid, have a short-ranged attractive interaction due to Van der Waals interaction. Therefore, in order to avoid particle aggregation, it is necessary colloidal suspensions to be stabilized electrostatically or sterically. Electrostatic stabilization creates repulsion between particles when they are charged by the repulsive Coulomb forces that may prohibit aggregation. Aggregation can then occur if salt is added in the suspension, therefore screening electrostatic repulsions or by altering pH. Steric stabilization of colloids is achieved by polymer attached to the particle surface and chains forming a coating, which creates a repulsive force when particles are suspended in good solvent for the polymers and separates the particle from another particle.

1.1 Hard sphere colloids

Colloidal hard spheres are ideally microscopic particles moving within a medium with Brownian motion that interact with an infinite repulsive potential when they touch. In particular, the interparticle potential of two hard sphere colloids is:

$$V(r) = \begin{cases} \infty & 0 < r < 2R \\ 0 & r > 2R \end{cases},$$

where R is the particle radius.

The phase behavior of hard spheres is independent of temperature. Therefore, considering only the entropy, the parameter to determine the phase behavior is the particle volume fraction Φ:

$$\Phi = \frac{4}{3}\pi R^3 \frac{N}{V}$$

Where N is the number of particles and V the total volume fraction.

Fig. 1.1 depicts the phase diagram of colloidal hard spheres. At volume fractions lower than 0.494, due to the Brownian motion, particles have a random distribution in the suspending fluid, resulting in a fluid state. A two-phase coexistence of fluid and crystal is observed at volume fraction ranging from 0.494 to 0.58 and a fully crystalline structure from 0.545 to 0.58[2]. The glass transition is around ~0.58 and can persist until a maximum packing fraction ~0.64, the random close packing[3]. The crystalline structure achieves a maximum packing as a face-centered crystal (FCC) at Φ_{fcc} =0.74.

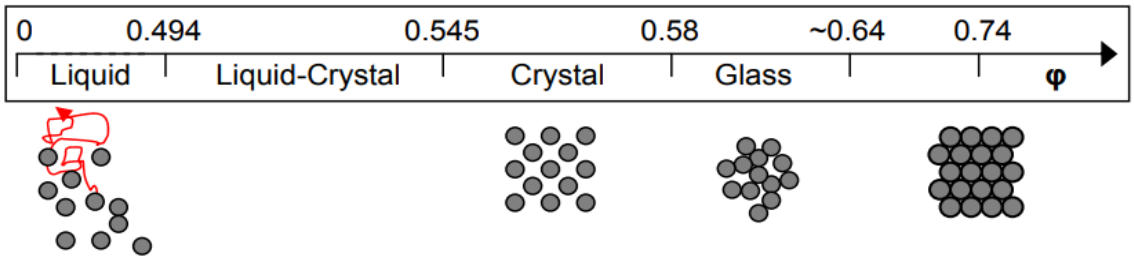

Figure 1.1 Hard sphere dispersion phase diagram

1.2 Depletion attractions

By the addition of non-adsorbing linear polymer, the repulsive potential of hard sphere colloids may be modified, resulting in a short-range attraction potential. In particular, the center of a polymer coil is excluded from a region around the hard sphere colloid at a range of approximately R_g , the polymer radius of gyration, leading to the increase of the free volume available to the polymer chains. According to the ideal model of Asakura and Oosawa[4], the attractive potential is proportional to the osmotic pressure of the polymer in solution and to the volume of the region between the particles from which polymer is excluded. Specifically, it depends on the concentration c_p of polymer in solution relative to the overlap concentration c_p^*, and on the radius of gyration R_g relative to the radius of colloid R, as:

$$\frac{U_{dep}(r)}{k_B T} = \begin{cases} \infty, & for\ r < 2a \\ \dfrac{c_p}{a c_p^*}\left(1+\dfrac{a}{R_g}\right)^3\left[1-\dfrac{3r}{4(a+R_g)}+\dfrac{r^3}{16(a+R_g)^3}\right], & for\ 2a < r < a+2R_g \\ 0, & for\ r > 2a+2R_g \end{cases}$$

1.3 Hard sphere colloidal gels

Altering the volume fraction φ or the interparticle potential $U(r)$ leads to a nonequilibrium dynamic arrest transition of the dispersed phase, resulting to a liquid to solid-like transition. At low volume fractions, particles are locally trapped by their attractive potential, leading to cluster formation, which, however, do not fill enough space and are free to diffuse. In order to exhibit solid-like properties, clusters must be trapped in a cage of neighboring cluster or directly connect to form a space-spanning network, where particles can reconfigure neither with respect to their nearest neighbors nor relative to any other particle within the network. The systems that fulfill both conditions for solid-like behavior, are the colloidal gels[5].

Gel formation occurs in the presence of attractive forces. There are two mechanisms to induce gelation: by ‘’strong’’ and by ‘’weak’’ interactions[5]. The ‘’strong’’ interactions refer to attractive Van der Waals forces, which are the forces that act between induced dipoles. In this work, the mechanism we use to form a gel is by ‘’weak’’ interactions: namely by depletion forces. Depletion gels are the most common model system that form gels via arrested phase separation, both at low and high densities. One main characteristic of those “nonequilibrium” gels is their coarsening via Brownian motion leading to aging that can be accelerated by shear or gravitational settling[1].

1.4 Tuning of colloidal gels

Tuning the properties of a colloidal gel is important to a wide range of industrial applications. This processing can occur by altering the concentration or the properties of particles or by changing the range or the strength of the inter-particle potential or other external conditions like temperature or pH. In this work, the mechanism we use to tune a gel is by shearing the system, which can produce a great variety of structures with different mechanical properties. Depending on the shear rate, various structural changes can occur such as clusters or strong bond breaking, not only in bulk, but also in two-dimensional[6] and microchannel flows[7]. Furthermore, recently, there have been done experiments of tuning of complex yield stress fluids induced by shear, described as a phenomenon of ‘’memory’’, as the system is believed to have retained a memory of its previous pre-shear history[8].

One method to shear a colloidal gel is by applying steady pre-shear. In this case, for an intermediate volume fraction depletion gel, it was found that at high shear rates the structure fully breaks into individual particles and after shear cessation leads to strong solid with homogeneous structure. At low shear rates, a largely inhomogeneous structure is created which remains stable after shear cessation and gives a weaker solid[9]. **Fig. 1.2** shows the results of a previous work of tuning colloidal gels by steady shear with rheo-confocal microscopy experiments, that enabled the microstructural changes to be captured.

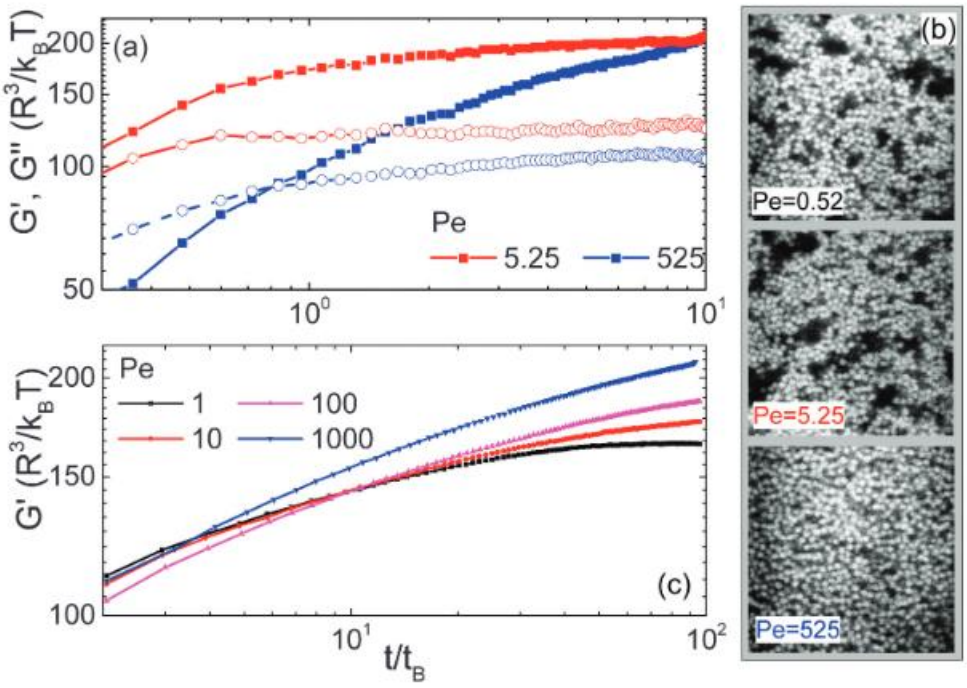

Figure 1.2. (a) Rheo-confocal experiments: time evolution of the linear viscoelastic moduli of a colloidal gel, with sphere radius $R = 830\ nm$, at $\omega = 1\ rad\ s^{-1}$, after cessation of shear rejuvenation at high and low shear rates, as indicated: G' (solid symbols) and G'' (open symbols); (b) the corresponding confocal images at $t = 10t_B$. (c) Rheological measurements of a similar colloidal gel at $\omega = 10\ rad\ s^{-1}$ with smaller spheres ($R = 400\ nm$) allowing the determination of long time behavior[9].

Shearing the same system oscillatory at large strain amplitudes leads to a stronger homogeneous gel because of the complete breakup of clusters, whereas at intermediate strain amplitudes a high heterogeneity occurs, resulting in a weak gel. This heterogeneity becomes weaker at lower strain amplitudes, where the depletion forces dominate related to the shear forces, and leads to a stronger gel[10]. The results of rheological experiments and BD simulations that occur by tuning colloidal gels by oscillatory shear are shown in **Fig. 1.3**.

Therefore, the oscillatory shear seems to be more efficient way to tune the mechanical properties of a colloidal gel as the steady shear does not produce as large heterogeneities in the structure as oscillatory shear does. On account of this, in this work we use oscillatory pre-shear to tune our sample.

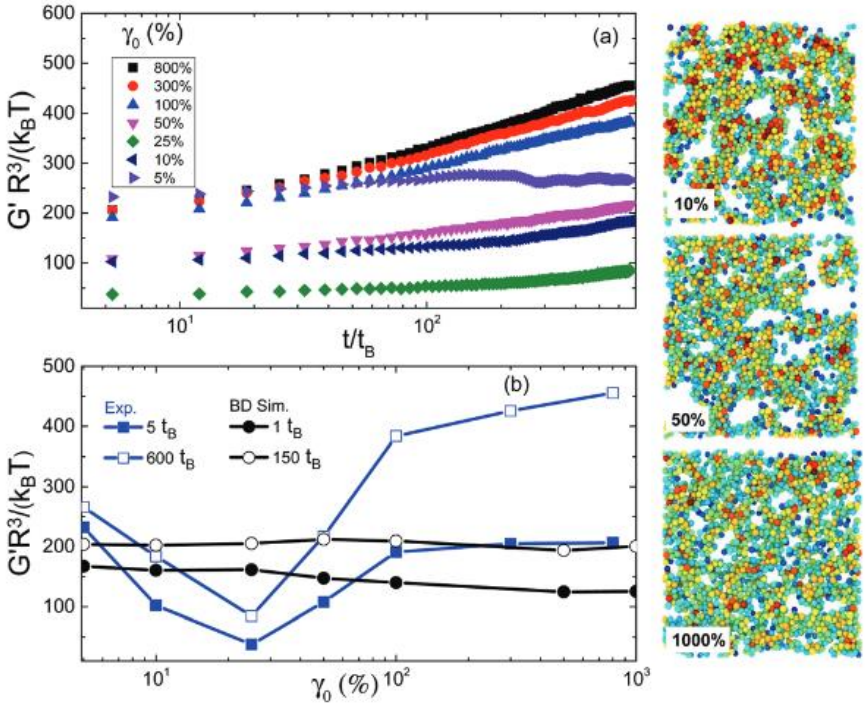

Figure 1.3. (a) Time evolution of the elastic modulus,G', measured in the linear viscoelastic regime from the experimental dynamic time sweep after oscillatory shear rejuvenation at different strain amplitudes as indicated, (b) G'versus the pre-shear strain amplitude at different times after flow cessation as indicated by both experiments and BD simulations. Images at the right depict structures produced by BD simulations at $100t_b$ after flow cessation.[10]

CHAPTER 2

SYSTEM AND TECHNIQUES

2.1 Sample preparation

The hard sphere particles used in this work consist of polymethylmethacrylate (PMMA) cores sterically stabilized by thin (≈10 nm) chemically grafted layers of poly-12-hydroxystearic acid (PHSA) chains. They are nearly monodispersed particles with hydrodynamic radius $R = 412\,nm$ .The particles are dispersed in squalene, a high boiling point solvent (b.p. 421.3℃) in order to avoid evaporation. Depletion attractions were implemented between the particles by adding non-adsorbing linear polybutadiene (1,4-addition) (PB) chains with a molecular weight, $M_w = 1243300\ g\ mol^{-1}$, a polydispersity index $M_w/M_n = 1.13$ and a radius of gyration, $R_g = 34\ nm$,measured by static light scattering. This implies a polymer–colloid size ratio $\xi = R_g/R = 0.08$ in dilute solution. We prepared the gel with an intermediate particle volume fraction $\varphi = 0.44$, and a polymer concentration $c_p/c_p^* = 0.65$, which gives an attraction strength at contact $U_{dep}(2R) = -20k_BT$ according to the modified Asakura-Oosawa model[4].

Colloidal gel preparation

The first step for sample preparation was to achieve random close packing at the colloidal suspension. To accomplish that, the sample was centrifuged until all colloids sedimented to the bottom and the sample was separated to the randomly close packed colloid and the floating solvent.

Polymer solution preparation

The next step was the preparation of the polymer solution. To achieve that, we first used the following equation to calculate the ratio of the mass of polymer solution m_{polsol} over the mass of colloidal suspension $m_{colsusp}$:

$$\varphi = \varphi_0 \left[1 + \frac{m_{polsol}}{m_{colsusp}} \left(1 + \frac{(x-1)\varphi_0}{1+ax}\right)\right],$$

where $x = \frac{\rho_c}{\rho_s}$, φ as the new volume fraction, φ_0 the old volume fraction, ρ_c the density of the colloid and ρ_s the density of the solvent. The parameter a is used to counterbalance the fact that the spheres have an increased radius when in solvent due to stabilizing layer. Here, the new volume fraction is $\varphi = 0.44$ and the old one is the volume fraction at random closed packing $\varphi_{rcp} = 0.64$. For the colloid $\rho_c = 1.118\ gr/cm^3$ for squalene, $\rho_{sq} = 0.8580\ gr/cm^3$. For a we used a typical value of $a = 0.12$.

We then used the following equation to calculate the concentration of polymers c at the polymer solution:

$$c_p = c\left[1 + \frac{m_{colsusp}}{m_{polsol}}\left(1 + \frac{(x-1)\varphi_0}{1+ax}\right)^{-1}\right]^{-1}$$

For the parameter c_p ,the modified Asakura-Oosawa model was used, which gave us the concentration of polymers needed for the attraction strength of $-20k_BT$.

Depletion gel preparation

Finally, the mix of the polymer solution with polymer concentration c and the colloidal suspension at volume fraction φ_{rcp} results to the depletion gel at volume fraction $\varphi = 0.44$ and attraction strength of$-20k_BT$.

2.2 Rheology - Background

Rheology is a science studying the deformation and the flow behavior of materials. The term originates from the Greek word "ροή" meaning "flow". Rheology has a wide range of applications to substances with complex microstructures such as polymers, suspensions, nanocomposites and to many materials of daily use such as foodstuffs, paints, additives, etc. The rheological properties of a material are measured by using rheometers. They measure the torque and the deflection angle of the measuring tool, while the rheological quantities, such as shear stress σ, deformation γ, shear rate $\dot{\gamma}$, are calculated from the measured values.

Fig. 2.1 shows the deformation geometry of simple shear. The area between the two flat rigid surfaces contains the material that is sheared. The ratio of the applied force F and the cross-sectional area of the surfaces A defines the shear stress σ:

$$\sigma = \frac{F}{A}$$

Shear strain γ is defined as the displacement of the top plate Δx over the thickness of the sample h:

$$\gamma = \frac{\Delta x}{h}$$

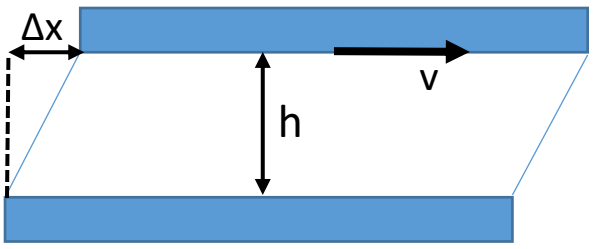

Figure 2.1 Two-dimensional representation of deformation in simple shear.

In the case where the material is perfectly elastic solid, the shear stress and the shear strain are proportional with a constant, known as the elastic modulus G:

$$\sigma = G \cdot \gamma \qquad \text{(}\textit{Hooke's Law of elasticity}\text{)}$$

On the other hand, if the material is a simple liquid, at any constant strain, the stress is zero. Thus, the stress is determined by the shear rate which, if the top plate moves with constant velocity, is the ratio of velocity v and the thickness of the sample h:

$$\dot{\gamma} = \frac{d\gamma}{dt} = \frac{v}{h}$$

In the case of simple liquids, the shear stress and the shear rate are proportional with another constant, defining the shear viscosity η:

$$\sigma = \eta \cdot \dot{\gamma} \qquad \text{(}\textit{Newton's Law of viscosity}\text{)}$$

The materials that behave like liquids at certain rates and as solids at others are known as viscoelastic materials.

Rheological measurements are divided in two categories: the steady shear flow and the oscillatory shear flow. In steady shear, a constant shear rate is applied to deform the material. It is a useful method in order to determine the yield stress of the sample, which is the stress above which the material flows. In oscillatory shear, instead of constant shear rate, a sinusoidal strain with angular frequency ω is applied at the sample:

$$\gamma(t) = \gamma_0 \sin(\omega t)$$

At low strain amplitudes (SAOS), the linear response of the material in terms of stress is given by the equation:

$$\sigma = \sigma_0 \sin(\omega t + \delta)$$

where δ is the phase lag. The storage modulus (G') and loss modulus (G'') are defined as ratios of stress and strain amplitudes. In particular, the storage modulus is based on amplitude of the in-phase stress and represents the solid-like response of the material. Loss modulus is based on the out-of-phase stress and represents the liquid-like response of the material. Thus, the linear response of the material can be represented by:

$$\sigma = \gamma_0 [G'(\omega) \sin(\omega t) + G''(\omega) \cos(\omega t)]$$

The ratio of storage and loss moduli is the tangent of the phase angle:

$$\tan \delta = \frac{G''}{G'}$$

At larger strain amplitudes (LAOS) the response of the material is nonlinear leading to large deformations, structural changes and possibly phase transitions (solid to liquid).

2.3 Confocal microscopy

Conventional optical microscopy can resolve individual colloidal particles of size ~1 μm, which is of order the wavelength of visible light, by using different techniques, such as bright field microscopy, dark field microscopy or differential interference contrast (DIC) microscopy. However, all those techniques are not ideal in the case of dense colloidal suspensions. Confocal microscopy is a useful technique for understanding colloidal dynamics and microstructure as it provides accurate information for the local structure and the dynamics in dense colloidal suspensions. **Fig. 2.2** demonstrates the working principle of a laser confocal scanning microscope (LCDM). There are two principal ideas: point by point illumination of the sample and rejection of out of focus light. The light from the laser is directed by a dichroic mirror towards a pair of mirrors that scan the light in x and y. Then it passes through the microscope objective causing excitation of the fluorescent sample. The light from the fluoresced sample then passes back through the objective and the pair of mirrors towards the dichroic mirror. The fluoresced light is followed by a pinhole placed in the conjugated focal (hence the name confocal) plane of the sample. The role of pinhole is to reject all the light coming from the out-of-focus planes. Finally, the light coming out of the pinhole is detected using a photomultiplier tube (PMT) detector[11].

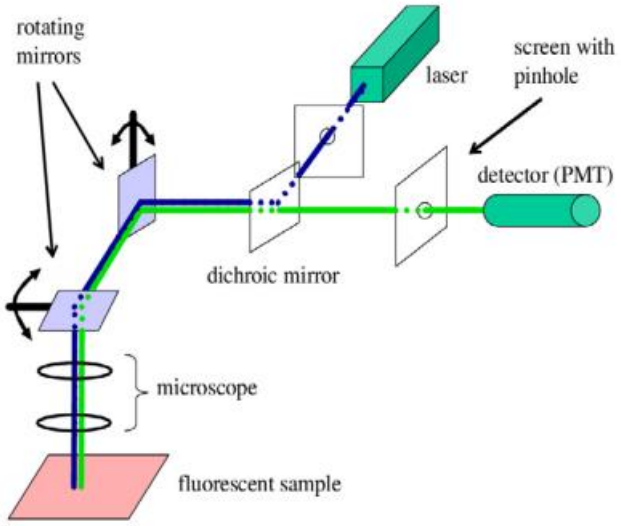

Figure 2.2: Working principle of a laser confocal scanning microscope (LCDM).

2.4 Experimental Setup

Sample Characterization

Rheology was measured at three different stress-controlled rheometers using various geometries. In all cases, the geometry was rough enough in order to avoid slip. More specifically, we used a) a MCR 501 Anton Paar rheometer with a geometry of homemade plastic cone-plate of diameter $25\ mm$, cone angle $2.79°$ and truncation $115\ \mu m$, b) a MCR702 Anton Paar rheometer with geometry of homemade cone-plate of diameter $40\ mm$, cone angle $2.3°$ and truncation $95\ \mu m$ and c) a MCR302 Anton Paar rheometer with geometry of

homemade cone-plate of diameter $40\,mm$, cone angle $2.54°$ and truncation $125\,\mu m$. Rheological measurements were performed at the suspension after a steady shear rejuvenation at $\dot{\gamma} = 500\,s^{-1}$ for $200\,sec$ after sample loading. Rejuvenation was followed by dynamic time sweep (DTS) test at $\gamma = 0.2\%$, $\omega = 1\,rad\,s^{-1}$ then a dynamic frequency sweep (DFS) at $\gamma = 0.2\%$ and $\omega = 100 - 0.1\,rad\,s^{-1}$ and finally a dynamic strain sweep (DSS) at $\gamma = 0.1 - 1000\%$ and $\omega = 1\,rad\,s^{-1}$. Furthermore, we performed high to low steady shear sweep to obtain a flow curve for the sample.

Pre-shear protocol

Here, all the measurements were performed at the rheometer MCR302 Anton Paar using rough geometry. The protocol we used to tune the gel is shown at **Fig. 2.3**. First, we performed a rejuvenation at $\dot{\gamma} = 500\,s^{-1}$ for $200\,sec$, stopping for $5\,sec$ $(\dot{\gamma} = 0)$ and then applying a DTS at $\gamma = 0.2\%$, $\omega = 1\,rad\,s^{-1}$ for $2000\,sec$ in order to achieve steady state. Subsequently, oscillatory pre-shears were performed at various strain amplitudes for different durations of time. The pre-shear was followed by DTS, DFS and DSS measurements.

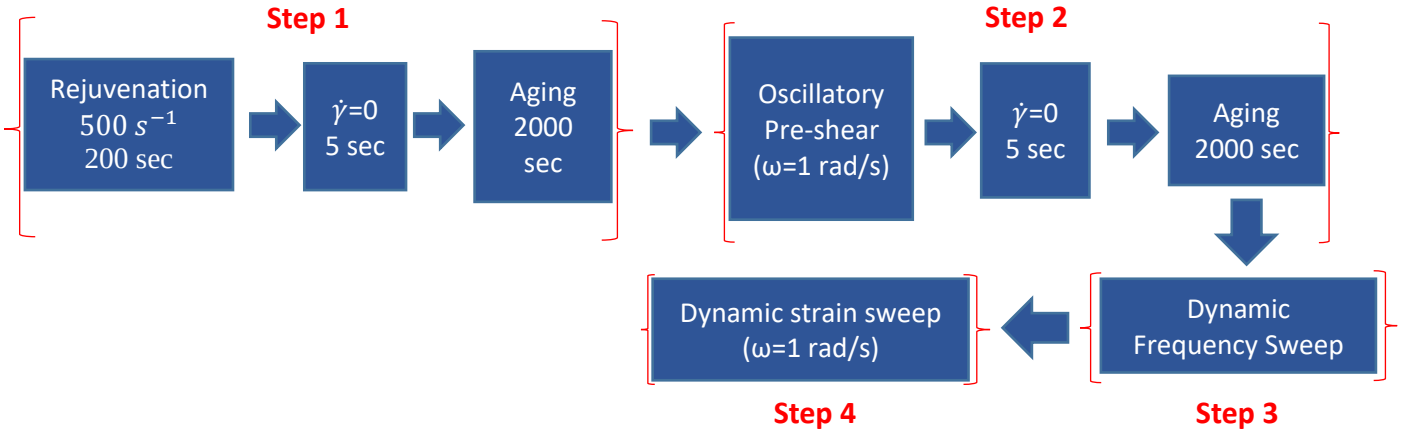

Figure 2.3: Tuning protocol of colloidal gel.

Furthermore, rheological measurements were performed using the same protocol but this time we directly sheared the sample after rejuvenation without performing the DTS of 2000 sec which serves as aging of the sample. This allows us to compare those two protocols and investigate the case where it may result in different microstructures and mechanical properties. The two protocols are compared in **Fig. 2.4** and the results will be presented in Chapter 3.

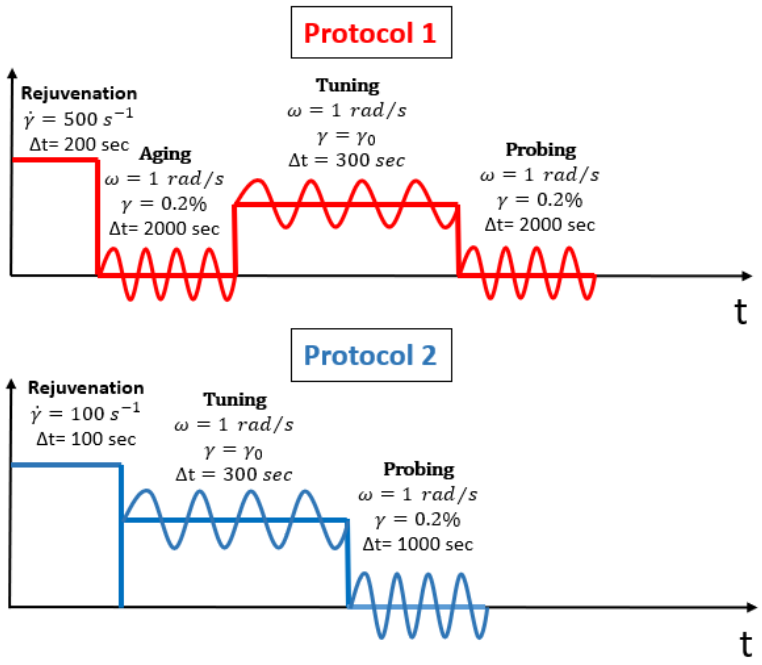

Figure 2.4: Two different protocols of tuning of colloidal gels.

Imaging protocol

In order to observe the microstructural changes of the gel under flow, we used a combination of confocal microscopy and rheometry. The microstructure was captured using an inverted microscope (TE Eclipse 300, Nikon) with a Confocal Scan Head (VTEye, Visitech) using a diode laser (λ=488 nm) scanning and piezo mounted objective (oil immersed, 100×, W. D. = 130 μm, Nikon). Furthermore, the rough bottom plate was replaced by a coverslip window coated with glass powder and we ensured that the new bottom plate did not affect the rheological measurements but allow direct observation of the sample.

CHAPTER 3

RESULTS

3.1 Linear viscoelasticity

The frequency dependence of G' and G'' in the linear regime is shown is **Fig. 3.1a**. DFS measurements show that the suspension exhibits solid-like behavior, when a slight increase with frequency of G' is observed. Furthermore, G'' shows a minimum that is related with the transition from α to β relaxation, within the Mode Coupling Theory (MCT) approach[12], or the characteristic time for the particle to explore its cage.

3.2 Nonlinear dynamic response

With the respect to the nonlinear dynamic response, the steady state values of the storage and loss moduli, G' and G'' as a function of the strain amplitude, γ, are shown in **Fig. 3.1b**. The dynamic strain sweep tests (DSS) were performed at three different frequencies ($\omega = 0.1, 1, 10\ rad \cdot s^{-1}$). First observation from our data is the appearance of a maximum of G'' which reflects the first yielding process and it is related to an inter-cluster bond-breaking[13]. We observe that the value of this maximum of G'' increases with frequency. However, a second yielding process is not detected at any of the three strain sweeps in contrast to previous findings in similar colloidal gels. A second observation is that by increasing the strain amplitude, a crossover of G' and G'' appears, beyond which the sample exhibits liquid-like response ($G'' > G'$). We notice that as the frequency increases the strain-crossover value decreases.

As it is mentioned at Experimental Setup (Chapter 2), we perform dynamic strain sweeps at frequency of $1\ rad\ s^{-1}$. Thus, the value of crossover-strain at this frequency is useful for the comparison with our next results. The crossover-strain value is the point at which the gel

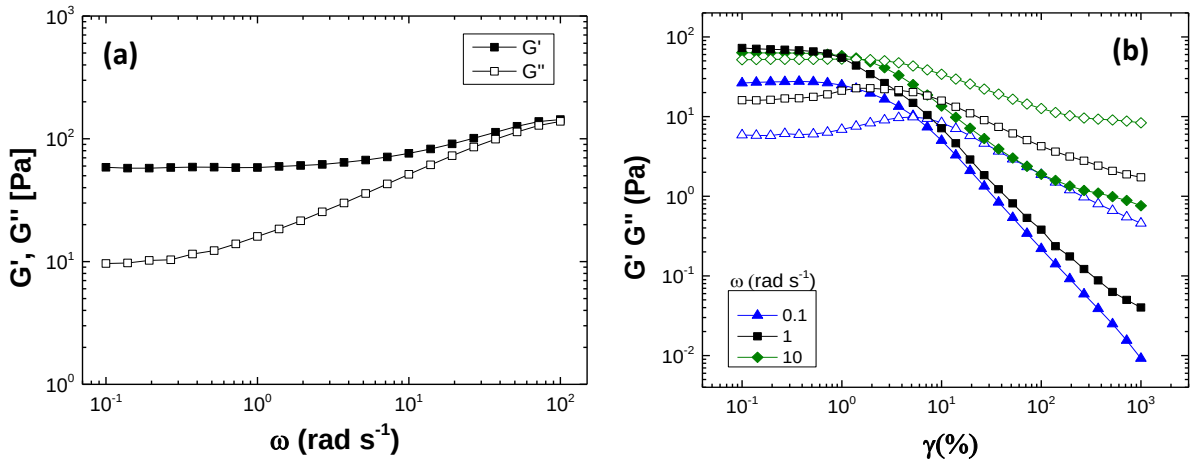

Figure 3.1. (a) DFS measurements at $\boldsymbol{\gamma = 0.2\%}$ and (b) DSS measurements performed at frequencies of $\boldsymbol{\omega = 0.1, 1, 10\ rad/s}$.

starts to exhibit nonlinear behavior in response to applied stress In **Fig. 3.1b**, we observe the crossover of G' and G'' is at strain amplitude of about 3%.

3.3 Steady shear response and yield stress

Next, we show the flow curve of the colloidal gel measured by performing a reverse constant shear rate sweep and measuring the stress response (**Fig. 3.2**). The suspension exhibits a shear thinning behavior and at low shear rates the flow curve seems to tend to yield stress plateau which is typical for a soft matter solid[14]. Above the yield stress the sample exhibits plastic flow with the stress increasing weakly with the shear rate.

In order to obtain the yield stress of the gel we fit our data with the expression:

$$\sigma = \sigma_y + \eta\dot{\gamma}^{\alpha}$$

where σ_y is the yield stress, η is the viscosity and α is a constant that can be lower or equal to 1. If $\alpha < 1$ the gel exhibit shear thinning behavior and the value of α represents the degree of this behavior, whereas if $\alpha = 1$ the sample exhibits Newtonian behavior. The values we get are: yield stress $\sigma_y = 1.022\ Pa$, viscosity $\eta = 2.16\ Pa \cdot s$ and $\alpha = 0.78 < 1$. The last result confirms the shear thinning behavior of our sample, although the fitting is not excellent. We believe that deviations at low shear rates can be due to possible slip or the fact that the gel might need longer time in order to reach steady state.

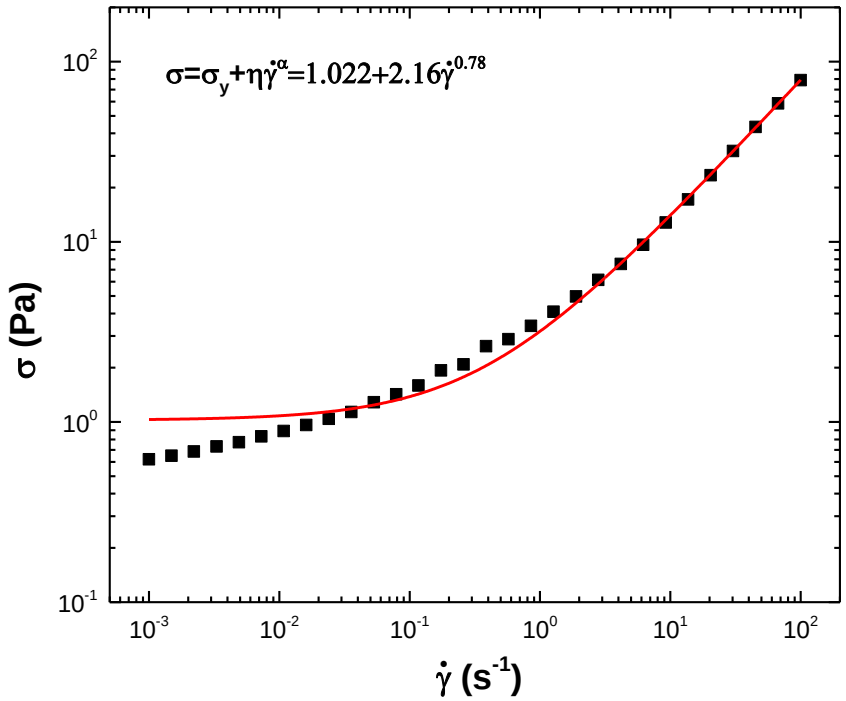

Figure 3.2. Flow curve of colloidal gel.

3.4 Response to pre-shear

After rejuvenation ($500\ s^{-1}$) and aging for $2000\ sec$ until steady state was reached, we subjected the colloidal gel to pre-shear protocol (oscillatory) and then measured the linear viscoelastic response (DTS and DFS measurements). Afterwards, the non-linear oscillatory response of the sample was probed by DSS measurements. This protocol was carried out at various strain amplitudes and for different durations of time (5 min, 30 min, 180 min, 360 min).

In **Fig. 3.3**, the DFS measurements after pre-shear at four strain amplitudes (3%, 10%, 70%, 300%) are shown and compared with the DFS measurement after rejuvenation. We observe that as the duration of pre-shear increases, the colloidal gel becomes weaker. In particular, 5 minutes shearing does not seem to affect efficiently the mechanical properties of the sample, whereas after increasing the duration at 30 minutes a slightly drop of moduli is observed which is more obvious at a pre-shear strain amplitude of $\gamma = 70\%$. This drop

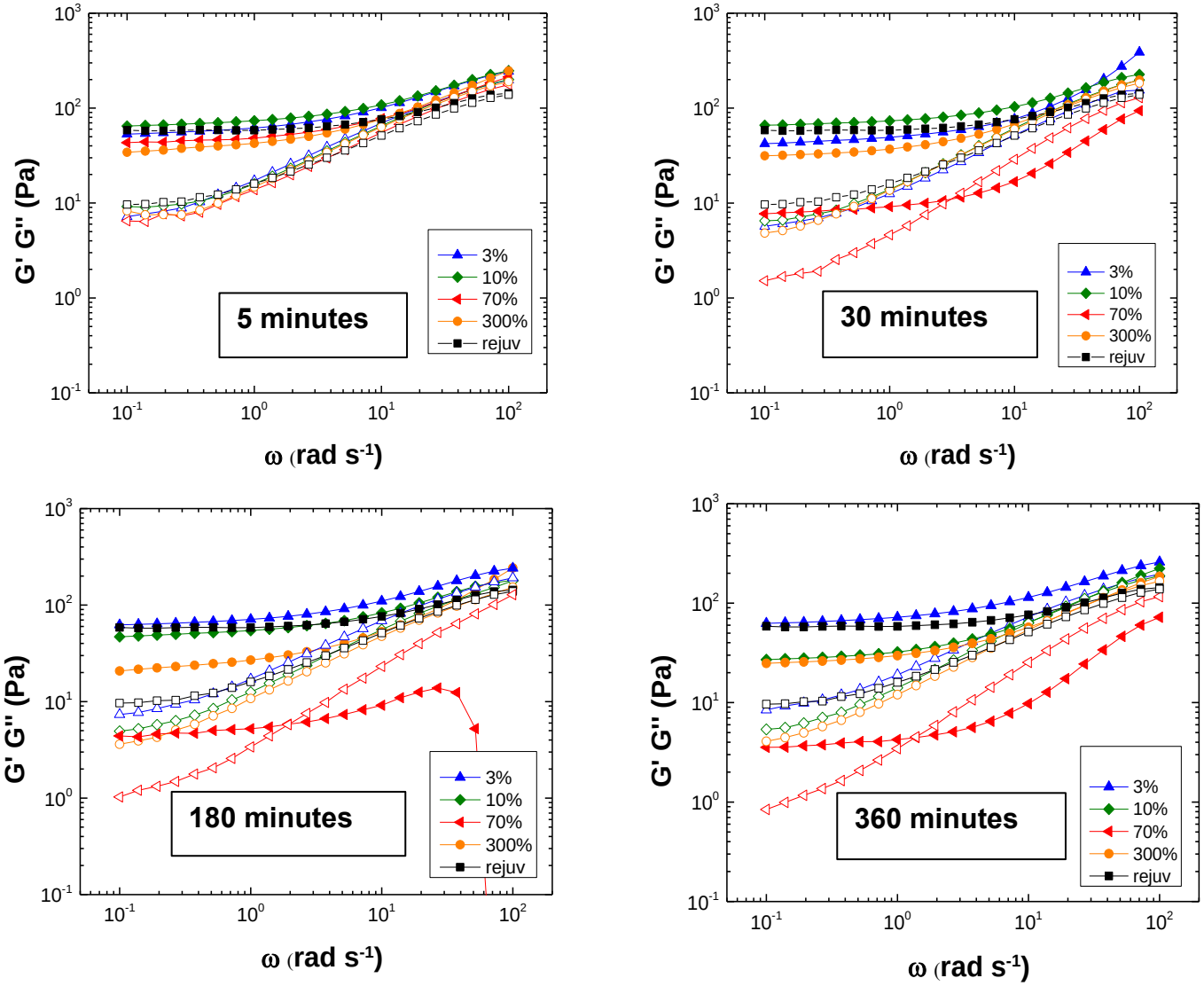

Figure 3.3. DFS measurements performed at γ=0.2%, after each pre-shear at strain amplitudes γ=3%, 10%, 70%, 300% compared with DFS measurement after rejuvenation.

becomes larger for shearing times of 180 and 360 minutes, suggesting that by altering the shearing time we observe changes in the structure and mechanical properties of the gel.

The response of colloidal gel at frequency sweep after rejuvenation shows that it exhibits solid-like behavior. However, after applying the pre-shear protocol at strain amplitude of $\gamma = 70\%$, a crossover of G' and G'' appears with the increase of the pre-shear duration. This means that at low shearing frequencies the sample's behavior is solid-like ($G' > G''$), while at higher frequencies, beyond the crossover, it exhibits liquid-like response ($G'' > G'$). This result indicates that a change in the microstructure may occur by pre-shear at this specific strain amplitude.

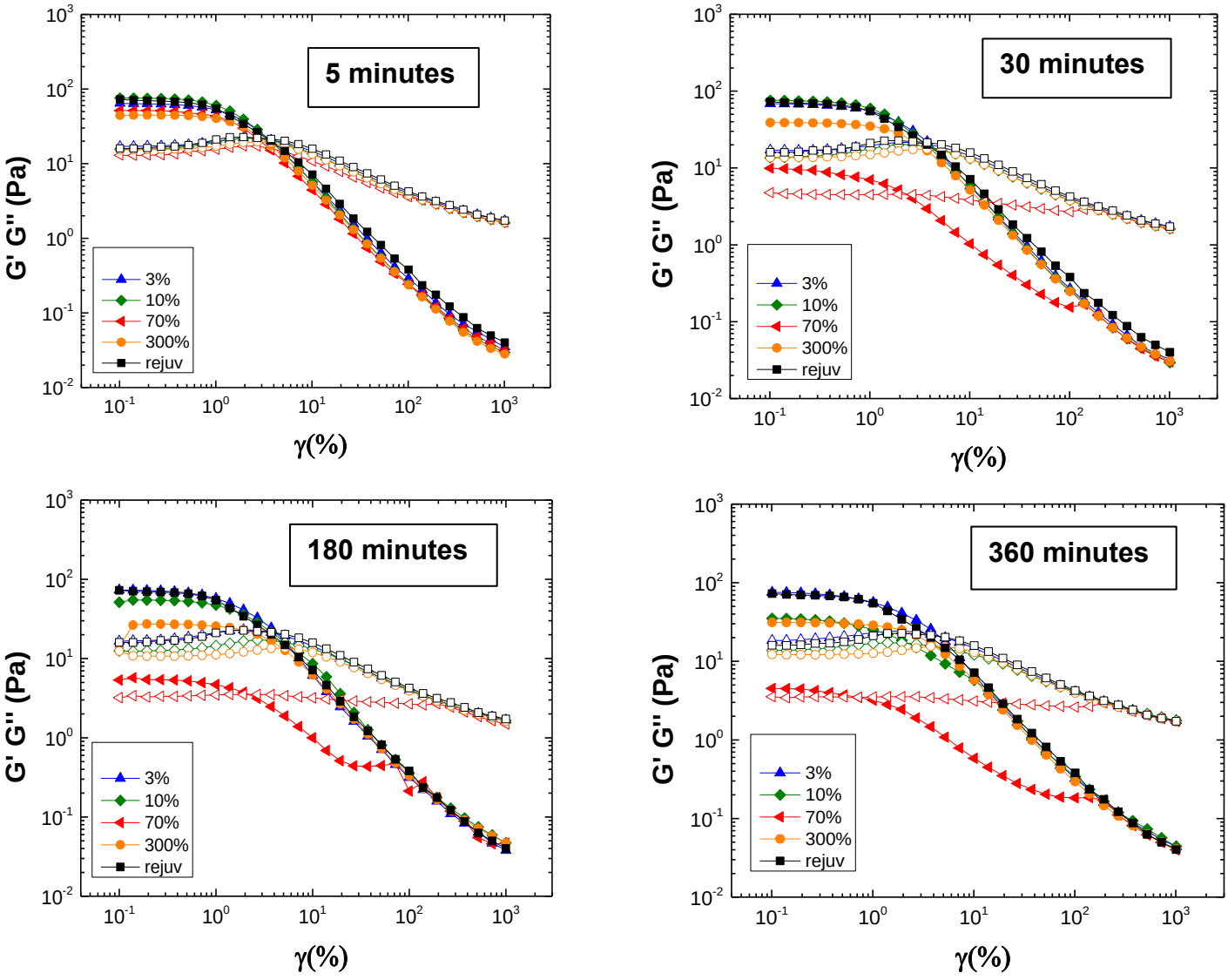

Figure 3.4. DSS measurements performed at $\boldsymbol{\omega = 1\, rad\, s^{-1}}$ after each pre-shear at various strain amplitudes γ=3%, 10%, 70%, 300% compared with DSS measurement after rejuvenation.

After monitoring the linear response of the colloidal gel we probe the extent of linear viscoelastic regime and the non-linear response by performing DSS measurements at $\omega = 1\ rad\ s^{-1}$ from $\gamma = 0.1\%$ to 100% (**Fig. 3.4**). First key observation made from those data is again the drop of moduli which becomes more obvious as the shearing time is increased, especially at strain amplitude of $\gamma = 70\%$. A second observation is related to the behavior of crossover-strain γ_c ($G' = G''$). Here, we focus on the weaker structure ($\gamma = 70\%$), observing that the γ_c is reduced as shearing time increases. As a third finding, focusing again on this strain amplitude, we observe that at shearing time of 30 minutes there is no peak of G'' and after longer time the gel exhibits a weaker solid-like behavior, as the distance of $G' - G''$ becomes smaller. Thus, we believe that the absence of the G'' peak is due to the fact that the gel is quite weak, with few interconnecting bonds between clusters that may smoothly break upon γ increase without much energy dissipation.

For the examination of the influence of pre-shear on the elastic modulus G', we normalize the values of G' after different pre-shear protocols, by the value of G' for the gel at quiescent state obtained after rejuvenation (G'_{Rej}). In **Fig. 3.5a**, we plot the normalized G' with the different strain amplitudes, for four different durations of pre-shears. We observe that as the strain amplitude of pre-shear increases, the gel becomes stronger ($G' > G'_{Rej}$), until a maximum value is reached. Shearing at intermediate strain amplitudes leads to a drop of normalized G', which becomes stronger as the shearing time increases. At high strain amplitudes, the gel shows a second maximum value and then again start decreasing. The weakest gel is created at strain amplitude of about $\gamma = 70\%$.

In order to better understand the relation of the gel microstructure with the mechanical properties, we follow the microstructure after shear cessation using combined rheology and confocal microscopy. Confocal images of the structure after different durations of pre-shearing time at $\gamma = 70\%$ are presented in **Fig. 3.5b**. The images reveal an inhomogeneous gel with the creation of larger clusters and voids as the shearing time increases. An important observation, is that a possible crystallization of the gel at shearing time of 360 minutes may occur, as the last confocal image reveals in Fig. 3.5b. In **Fig. 3.6**, we highlight in this duration of shearing time, presenting confocal images taken after pre-shear at various strain amplitudes. On the right side of the figure, we see the percolated network that is formed when the gel is at quiescent state. At strain amplitudes of $\gamma = 3\%, 200\%, 1000\%$ we don't observe any obvious structural changes on the gel's microstructure, but only on mechanical properties, as we discussed before. Nevertheless, applying pre-shear at $\gamma = 70\%$ for 360 minutes causes both structural and mechanical changes, leading to a structure with larger clusters and void, that can be related with crystallization of the gel, as the images show.

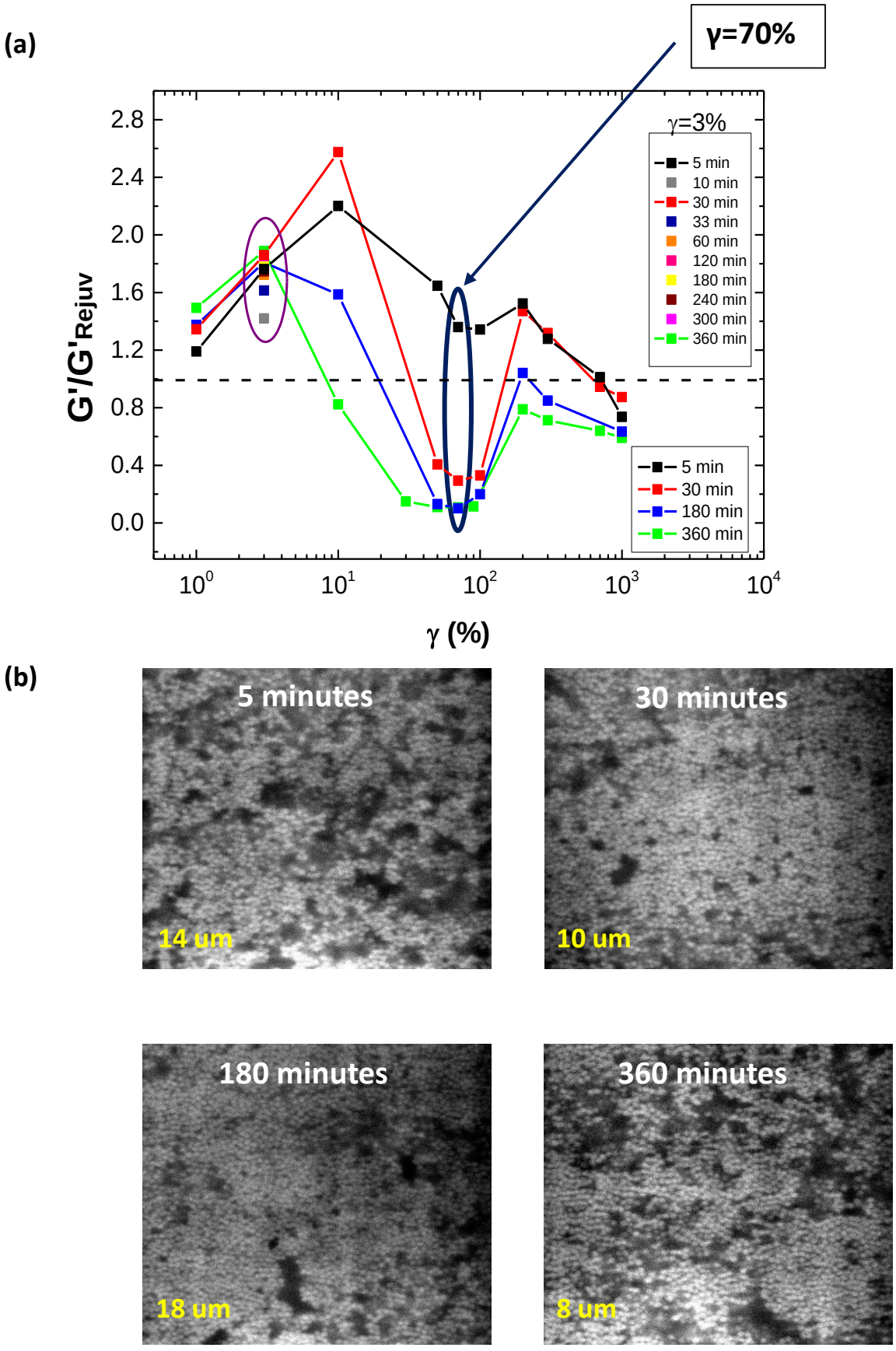

Figure 3.5. (a) G' obtained after aging of colloidal gels that underwent oscillatory pre-shear. G' here is normalized by G' of gel after rejuvenation. (b) Confocal images of structure after pre-shear at 70% for different shearing time. The position of the image relative to bottom plate is also indicated.

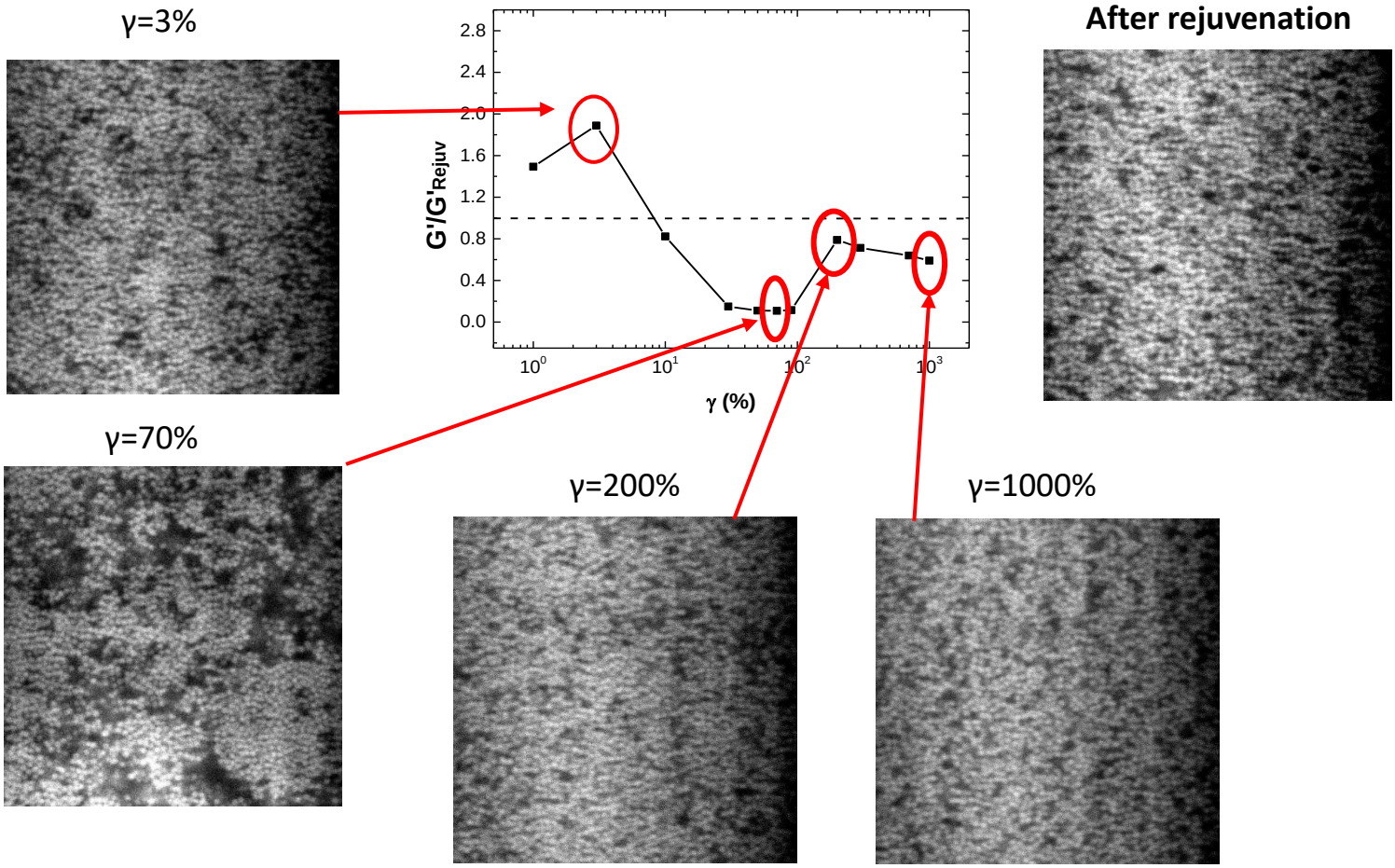

Figure 3.6. Confocal images of structure after applying pre-shear protocol for 360 minutes.

Next, we focused on the strain amplitude of $\gamma = 3\%$, where the crossover of G' and G'' was observed (**Fig. 3.2**). We applied pre-shear for further durations of time as is shown at the diagram in **Fig 3.5a**. We observe that the increase of shearing time leads to the increase of normalized G'. This is more obvious in **Fig. 3.7**, which shows the normalized G' plotted with the pre-shearing time. These results reveal that at some point the increase of normalized G' with pre-shearing time stops and at this point the gel has obtained a certain structure which is stable for longer shearing times.

Another parameter that may affect the tunability of the colloidal gel is the oscillatory frequency of pre-shear. We repeated the pre-shear protocol with shearing time of 180 minutes, at a frequency of $\omega = 10\, rad/s$. In **Fig. 3.8**, we compare the rheological results of tuning in those two frequencies ($\omega_1 = 1\, rad/s$ and $\omega_2 = 10\, rad/s$). At low strain amplitudes the frequency of ω_1 make a stronger gel while at high strain amplitudes the frequency ω_2 seems more efficient in strengthening of the gel. Furthermore, we observe that shearing at intermediate amplitudes causes a bigger drop of normalized G' at lower frequencies $(\omega_1 = 1\, rad/s)$, resulting to a weaker gel. Here further investigation by rheo-confocal experiments is required to provide us with additional information about the microstructural changes induced at different frequencies and their link to the mechanical properties.

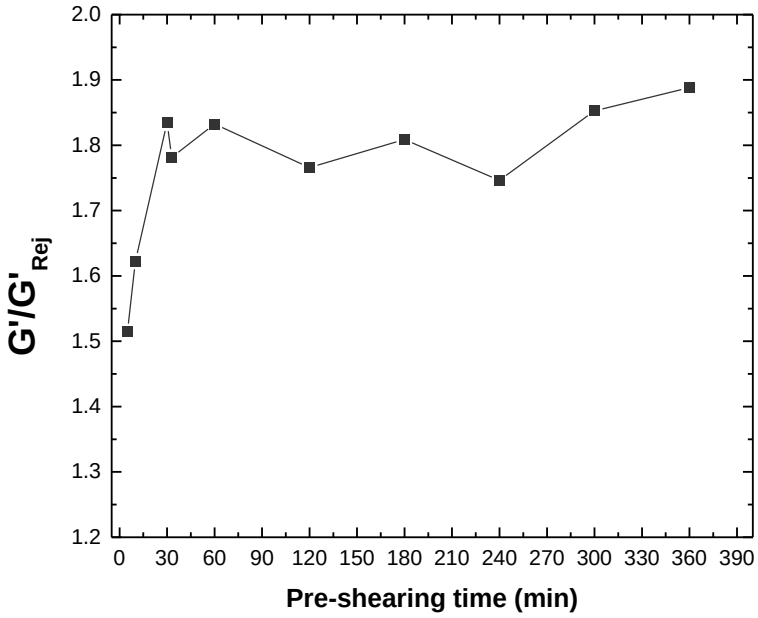

Figure 3.7. Storage modulus vs shearing time at γ=3%

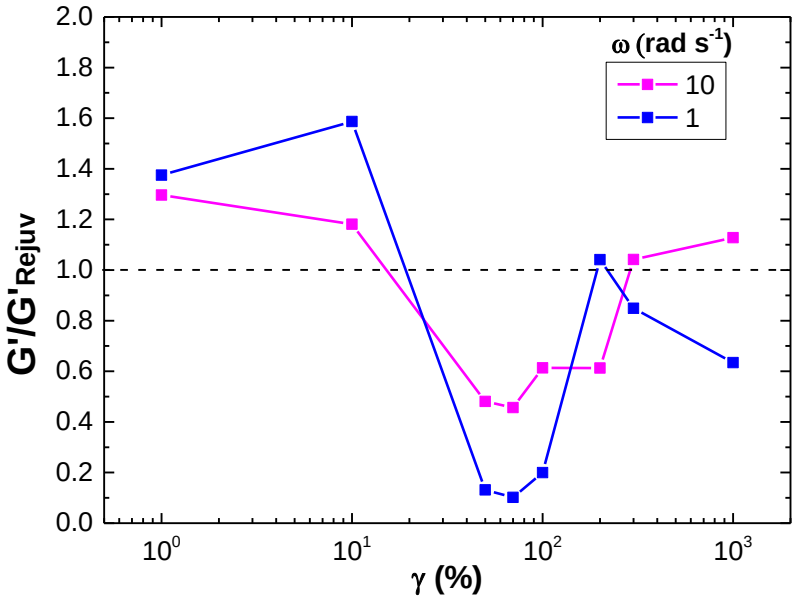

Figure 3.8. Storage modulus vs frequency (180 min pre-shear)

Finally, in **Fig. 3.9** we compare the effects on the mechanical properties by applying pre-shear using the two different protocols. The two protocols are presented on the right side of Fig. 10, (also more detailed in Fig. 2.4, Chapter 2). The protocol 1 is the one that we used in all our previous measurements. We first rejuvenate the sample at $\dot{\gamma} = 500\, s^{-1}$ for 200

seconds, then applying DTS for 2000 seconds until steady state is reached. Afterwards, the sample was pre-sheared for 300 seconds at various strain amplitudes and probed for 2000 seconds. The difference in the second protocol (protocol 2) is the absence of DTS after rejuvenation, as we pre-shear the gel directly after rejuvenation. We observe that at low strain amplitudes protocol 1 creates a slightly stronger gel, when at higher pre-shear strain amplitudes the gel is weaker using protocol 1 than protocol 2. Thus, giving time to the gel to reach the steady state after rejuvenation results in quite different mechanical properties compared to what extent with the case of shearing directly after rejuvenation. In future studies, we can investigate if the application of those two different protocols lead also to different microstructural changes.

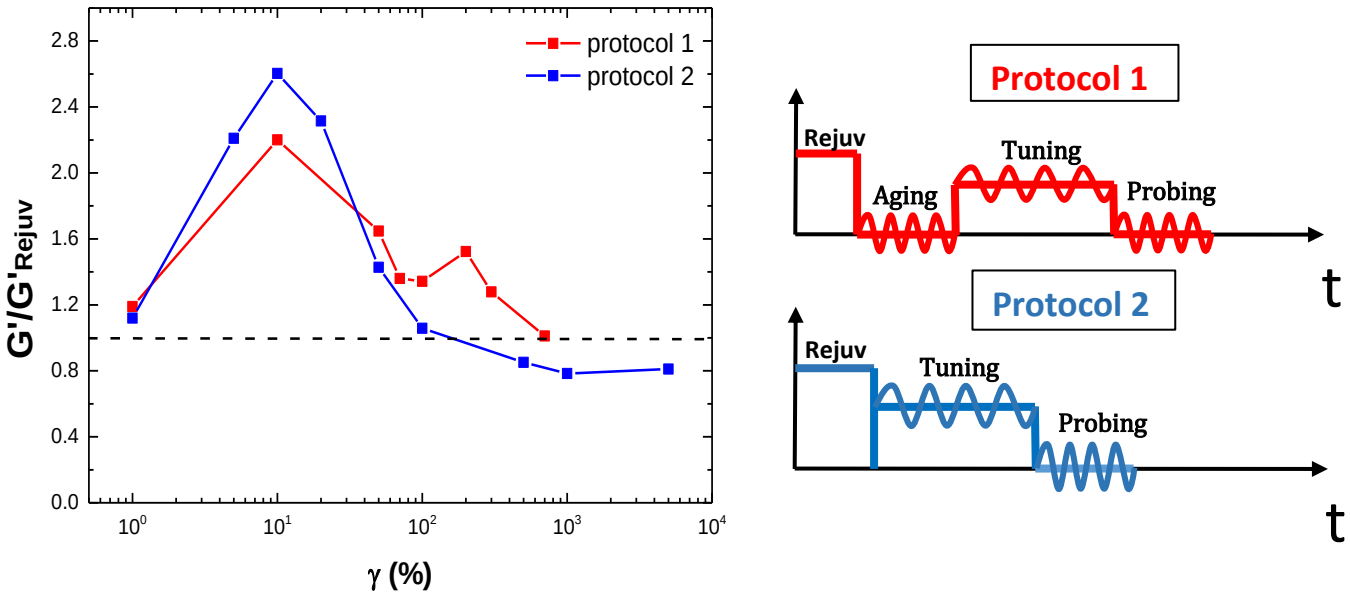

Figure 3.9. Comparison of two different pre-shear protocols (5 min) : (1) with aging after rejuvenation and (2) without aging after rejuvenation.

3.5 Conclusions

In summary, we have investigated the linear viscoelasticity and the nonlinear rheological response of colloidal gels subjected to two different oscillatory pre-shear protocols as well as the underlying changes in structure of the gel consisted of PMMA particles suspended in squalene with the addition of non-absorbing polymer. We show that after applying oscillatory pre-shear, a maximum drop of storage modulus (G') is observed at strain amplitude of $\gamma = 70\%$, which depends on the pre-shearing time. As the shearing time increases, the drop becomes larger and by using rheo-confocal technique, we found that this drop is related to the crystallization of the gel's clusters. Next, we observed that this protocol at the crossover-strain $\gamma_c = 3\%$ induces strengthening effects that are also time-dependent. In addition, we found that there is also a frequency dependence on mechanical response after applying pre-shear. Lastly, we observed that shearing the gel directly after rejuvenation results in different response compared with the first pre-shear protocol we used. The last two findings can be

further investigated in future measurements, using also rheo-confocal microscopy, in order to examine the structural changes that may occur.

Appendix 1: Reproducibility check using different geometries

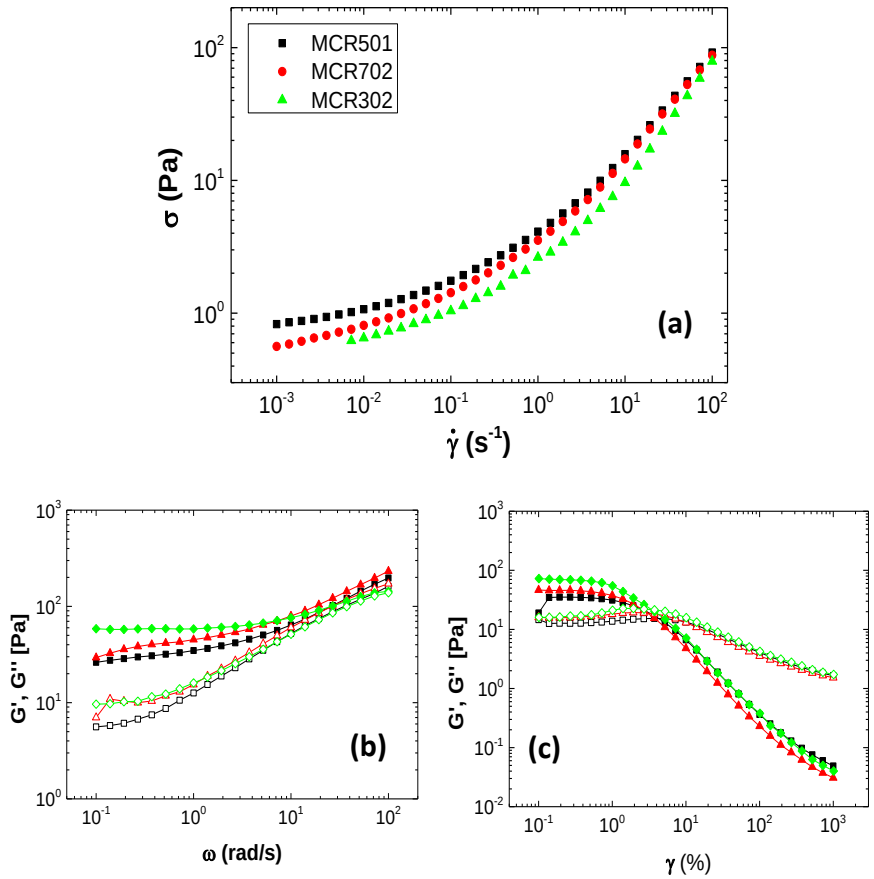

Figure 3.10. Sample characterization measured by three different rheometers. (a) Shear stress as a function of shear rate starting from higher rates to lower. (b) Dynamic frequency sweep at strain amplitude $\gamma = 0.2\%$. (c) Storage modulus G' (solid symbols) and loss modulus G''(open symbols) as a function of shear strain at frequency $\omega = 1\ \mathrm{rad/s}$.

In order to ensure the reproducibility of the sample response, we carried out rheological measurements using three rheometers with different rough geometries, as is detailed in Experimental Setup, (Chapter 2). The rheological measurements we performed were flow curve, dynamic strain sweeps (DSS) and dynamic frequency sweeps (DFS) using the same protocol as discussed for the previous experiments. In **Fig. 3.10**, we compare the results we took from the three rheometers (MCR302, MCR501, MCR702). We observe that there is a slightly difference which is more obvious at MCR302 compared to the other two rheometers. We believe that those differences can be related to the calibration of each rheometer, because even minor differences in the calibration can affect the accuracy of our measurements. In addition, the use of cone-plate geometries with different angle and truncation can have a significant impact on our measurements. Thus, the combination of those two factors could be the reason of variations in our results. For the appliance of pre-

shear protocol, we chose to use the MCR302, in order to be able to perform rheo-confocal measurements.

Appendix 2: Searching for effective rejuvenation

	(1)	(2)	(3)
Rejuvenation (steady shear)	$\dot{\gamma} = 100\ s^{-1}$ $\Delta t = 400\ sec$	$\dot{\gamma} = 200\ s^{-1}$ $\Delta t = 200\ sec$	$\dot{\gamma} = 500\ s^{-1}$ $\Delta t = 200\ sec$
Deviation	~20%	~15%	~7%

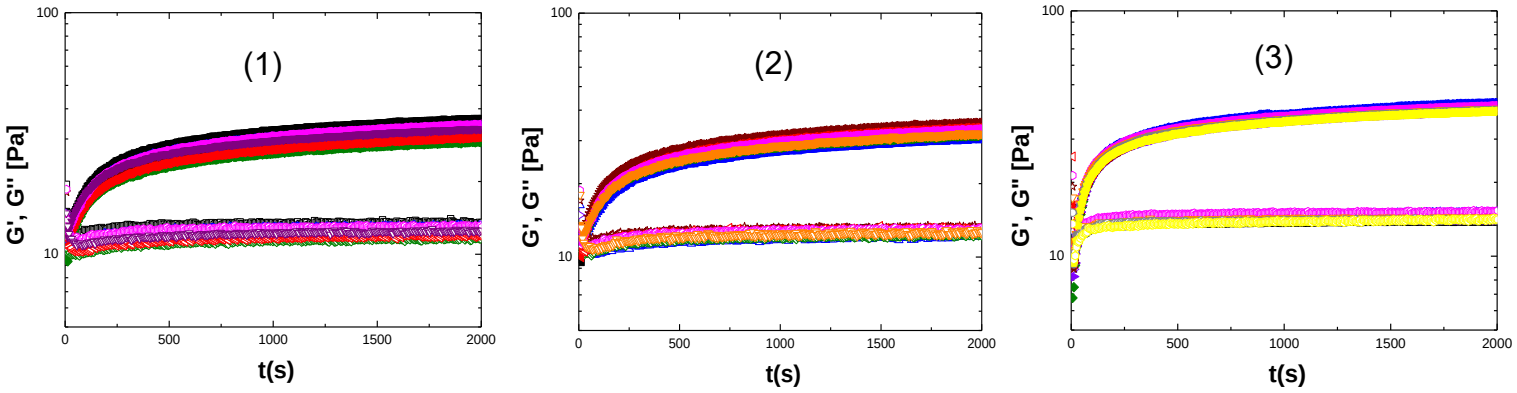

Figure 3.11. Time evolution of colloidal gel after different rejuvenation.

Before the investigation of the effects that a pre-shear protocol can induce in a colloidal gel, it was important to search for the most effective rejuvenation protocol for our sample. The table in **Fig. 3.11** shows the three different rejuvenations we tried, whereas the diagrams below are the time evolution of the gel after each rejuvenation. An effective rejuvenation protocol would be the one that gives the smallest deviation on moduli between consequtive measurements. As we observed, the first protocol ($\dot{\gamma} = 100\ s^{-1}, \Delta t = 400\ sec$) leads to large deviation of moduli (~20%). Thus, we increased the shear rate and decrease the duration of shearing (2nd protocol: $\dot{\gamma} = 200\ s^{-1}, \Delta t = 200\ sec$). The deviation, in this case, was smaller(~15%). The final rejuvenation protocol that turned out to be the most effective compared with the previous two and the one we used for our pre-shear protocol, was at shear rate of $\dot{\gamma} = 500\ s^{-1}$ for $\Delta t = 200\ sec$, with deviation of moduli ~7%.

References

1. J. Mewis, N. J. W. *Colloidal suspension rheology*. *Cambridge University Press* vol. 7 (2012).

2. P. N. Pusey & Megen, W. van. Phase behaviour of concentrated suspensions of nearly colloidal spheres. *Nature* 2–4 (1986).

3. Schaertl, W. & Sillescu, H. Brownian dynamics of polydisperse colloidal hard spheres: Equilibrium structures and random close packings. *J Stat Phys* **77**, 1007–1025 (1994).

4. Asakura, S. & Oosawa, F. On interaction between two bodies immersed in a solution of macromolecules. *J Chem Phys* **22**, 1255–1256 (1954).

5. Fernandez-Nieves, A. & Puertas, A. M. Fluids, Colloids and Soft Materials: An Introduction to Soft Matter Physics. *Fluids, Colloids and Soft Materials: An Introduction to Soft Matter Physics* 1–408 (2018) doi:10.1002/9781119220510.

6. Masschaele, K., Fransaer, J. & Vermant, J. Direct visualization of yielding in model two-dimensional colloidal gels subjected to shear flow. *J Rheol (N Y N Y)* **53**, 1437–1460 (2009).

7. Conrad, J. C. & Lewis, J. A. Structure of colloidal gels during MicroChannel flow. *Langmuir* **24**, 7628–7634 (2008).

8. Schwen, E. M., Ramaswamy, M., Cheng, C. M., Jan, L. & Cohen, I. Embedding orthogonal memories in a colloidal gel through oscillatory shear. *Soft Matter* **16**, 3746–3752 (2020).

9. Koumakis, N. *et al.* Tuning colloidal gels by shear. *Soft Matter* **11**, 4640–4648 (2015).

10. Moghimi, E., Jacob, A. R., Koumakis, N. & Petekidis, G. Colloidal gels tuned by oscillatory shear. *Soft Matter* **13**, 2371–2383 (2017).

11. Prasad, V., Semwogerere, D. & Weeks, E. R. Confocal microscopy of colloids. *Journal of Physics Condensed Matter* **19**, (2007).

12. Mason', T. G. & Weitz', D. A. *Linear Viscoelasticity of Colloidal Hard Sphere Suspensions near the Glass Transition*. vol. 75 (1995).

13. Koumakis, N. & Petekidis, G. Two step yielding in attractive colloids: Transition from gels to attractive glasses. *Soft Matter* **7**, 2456–2470 (2011).

14. Laurati, M., Egelhaaf, S. U. & Petekidis, G. Nonlinear rheology of colloidal gels with intermediate volume fraction. *J Rheol (N Y N Y)* **55**, 673–706 (2011).